NANO LETTERS

Letter

pubs.acs.org/NanoLett

A Comparative Study of Absorption in Vertically and Laterally Oriented InP Core–Shell Nanowire Photovoltaic Devices

Ali Nowzari,[†] Magnus Heurlin,[†] Vishal Jain,[†,‡] Kristian Storm,[†] Ali Hosseinnia,[†] Nicklas Anttu,[†] Magnus T. Borgström,[†] Håkan Pettersson,[†,‡] and Lars Samuelson[†,*]

[†]Division of Solid State Physics and The Nanometer Structure Consortium (nmC@LU), Lund University, Box 118, 22100 Lund, Sweden

[‡]Laboratory of Mathematics, Physics and Electrical Engineering, Halmstad University, Box 823, SE-30118 Halmstad, Sweden

Supporting Information

ABSTRACT: We have compared the absorption in InP core–shell nanowire p–i–n junctions in lateral and vertical orientation. Arrays of vertical core–shell nanowires with 400 nm pitch and 280 nm diameter, as well as corresponding lateral single core–shell nanowires, were configured as photovoltaic devices. The photovoltaic characteristics of the samples, measured under 1 sun illumination, showed a higher absorption in lateral single nanowires compared to that in individual vertical nanowires, arranged in arrays with 400 nm pitch. Electromagnetic modeling of the structures confirmed the experimental observations and showed that the absorption in a vertical nanowire in an array depends strongly on the array pitch. The modeling demonstrated that, depending on the array pitch, absorption in a vertical nanowire can be lower or higher than that in a lateral nanowire with equal absorption predicted at a pitch of 510 nm for our nanowire geometry. The technology described in this Letter facilitates quantitative comparison of absorption in laterally and vertically oriented core–shell nanowire p–i–n junctions and can aid in the design, optimization, and performance evaluation of nanowire-based core–shell photovoltaic devices.

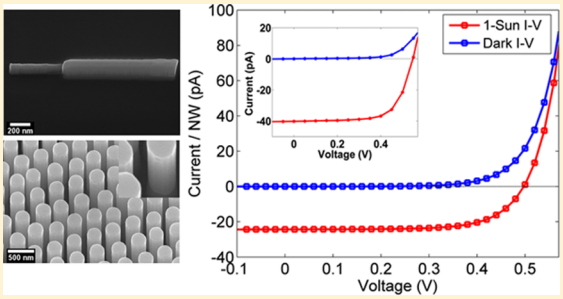

KEYWORDS: *Nanowire, absorption, solar cell, photovoltaics, core–shell, radial, InP*

Semiconductor nanowires (NWs) are promising building blocks for next-generation photovoltaics.[1−5] The nanoscale dimensions of NWs provide strain relaxation capability, enabling heteroepitaxy of III–*V* materials on Si as well as a higher degree of freedom in the design of multijunction solar cells with lattice-mismatched materials.[6,7] The subwavelength dimensions of NWs together with their large surface-to-volume ratio, and the possibility of being grown in the form of a periodic array with a predetermined pitch, give NWs the potential to enhance optical absorption.[8−10] The strain relaxation property and the enhanced absorption cross section combined make NWs potential candidates for the realization of highly efficient, low-cost solar cells.[1]

Apart from the NW material composition, light absorption in NWs depends strongly on the dimensions, arrangement and orientation of NWs with respect to the incident light.[11−13] This geometry-dependent absorption, being highly influenced by resonances and waveguiding effects, arises from the interaction of light with objects having dimensions comparable to the wavelength of the incident light. The interaction of light with NWs is dominated by diffraction, which can result in constructive interference within the NWs, leading to absorption resonances.[14]

There are a number of reports in the literature on the absorption and photovoltaic (PV) properties of vertically or laterally oriented NWs in different semiconductor materials with axial or radial p–n junctions.[13,15,16] However, a quantitative comparison of the performance of vertically and laterally oriented NW PV devices is lacking. In this work, we present a comparative study of the absorption of light in laterally oriented single InP core–shell NW PV devices and corresponding identical NWs in vertically oriented arrays with 400 nm pitch.

InP NWs were grown using a two-step core–shell growth method to facilitate the comparison of absorption in laterally and vertically oriented NWs. We note that the conventional method of electrically contacting the core in a lateral single core–shell NW is based on selectively etching the shell to expose the core for the deposition of the contact.[17] This contacting method reduces the junction length that in turn makes the direct quantitative comparison of absorption in such a NW with that in a corresponding unetched vertical NW questionable. In addition, selective etching of the shell can be complicated when there is no proper selective etchant available for the shell with respect to the core material. In order to address these problems in the comparison of absorption and device fabrication, we performed the core and shell growth in

Received: November 27, 2014
Revised: January 30, 2015
Published: February 11, 2015

DOI: 10.1021/nl504559g
Nano Lett. 2015, 15, 1809−1814

two separate steps. This two-step growth method allows adding a sacrificial SiO_2 shell to the bottom part of the core before the growth of InP shells, which preserves the NW geometry in the lateral single NW contacting process, thus enabling the attempted direct comparison of absorption in vertically and laterally oriented NWs. The intended NW structure is depicted in the schematic in Figure 1, and the details of the actual NW growth are described below.

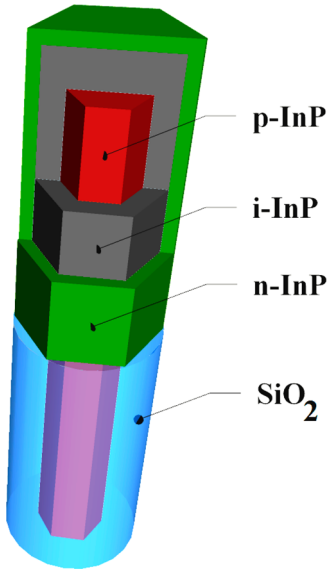

Figure 1. Schematic of a p−i−n core−shell NW structure with shells grown only on the top part of the core, enabling a quantitative direct comparison of absorption in lateral single and vertical array PV devices.

InP NW cores and shells were grown in an Aixtron 200/4 metal−organic vapor phase epitaxy (MOVPE) machine with a total flow of 13 L/min, working pressure of 100 mbar, and with H_2 as the carrier gas. The growth substrates consisted of p-type InP 111B wafers covered with a 20 nm thick SiN film in which periodic openings with 400 nm pitch were patterned using nanoimprint lithography (NIL) and reactive ion etching (RIE). Au seed particles were positioned inside the SiN film openings on the substrates by thermal evaporation of gold and lift-off on the existing NIL-patterned polymers used in the RIE patterning step.[18] The precursors used for the growth were trimethylindium (TMIn), phosphine (PH_3), diethylzinc (DEZn), tetraethyltin (TESn), and hydrogen chloride (HCl). In the first step, InP NW cores were grown in VLS[19] mode from the Au particles at a temperature of 440 °C using the following precursor molar fractions: $\chi_{TMIn} = 7.4 \times 10^{-5}$, $\chi_{PH3} = 6.9 \times 10^{-3}$, $\chi_{DEZn} = 5.3 \times 10^{-5}$, $\chi_{TESn} = 1.2 \times 10^{-6}$, and $\chi_{HCl} = 6.1 \times 10^{-5}$. Growth was initiated by a 15 s p-type nucleation step without HCl and with $\chi_{PH3} = 2.3 \times 10^{-3}$. The p-, i- and n-type segments of the NW cores were grown for 4.0, 5.0, and 2.5 min, respectively, resulting in 2 μm tall NWs with 500 nm i- and n-segments, and with a diameter of 130 nm. The axially grown i- and n-type segments were added to the p-cores to ensure enough i- and n-type material deposition on top of the NW cores, necessary to avoid leakage current from the top of the cores in the subsequently fabricated p−i−n devices. The NW cores were then covered with a 75 nm thick shell of SiO_2 using atomic layer deposition (ALD), followed by an approximately 2 nm thick ALD-deposited aluminum oxide (Al_2O_3). The aluminum oxide shell was deposited on top of the SiO_2 layer to increase the adhesion between the oxide and the resists, used in the subsequent processing steps. Next, the samples were coated with a resist and underwent RIE in order to expose the top parts of the NWs. Following this, the samples were etched in a buffered HF solution, resulting in NWs with oxide shells that only covered the bottom 0.9 μm part of the cores as seen in the scanning electron microscope (SEM) image in Figure 2a. Then, the Au particles were removed from the top of the NWs with wet chemical etching to suppress axial growth.[20] The NW cores were subsequently reinserted into the MOVPE reactor for the growth of the nominally intrinsic and n-doped shells at a temperature of 575 °C using molar fractions of $\chi_{TMIn} = 6.5 \times 10^{-5}$ and $\chi_{PH3} = 11.5 \times 10^{-3}$ for the nominally intrinsic shell and $\chi_{TMIn} = 6.5 \times 10^{-5}$, $\chi_{PH3} = 0.77 \times 10^{-3}$, and $\chi_{TESn} = 2.4 \times 10^{-6}$ for the n-type shell. The growth times were 12 and 4.5 min resulting in approximate thicknesses of 55 and 20 nm for the i- and n-type shells, respectively. The carrier concentration in the n-type shell has previously been measured in a similar structure to be 3×10^{19} cm^{-3}, which facilitates the formation of a low resistance ohmic contact.[18] The presence of the oxide shell during the shell growth resulted in material growth, occurring only on the top uncovered part of the NW cores. The final NW structure thus consisted of a radial p−i−n junction of 280 nm in diameter on the top 1.1 μm part of the cores, while the bottom part consisted of a p-type core covered with an oxide shell as shown in the SEM image in Figure 2b. For probing lateral single NW core−shell devices, this growth method enables a noninvasive access to the core after etching of the bottom oxide shell without altering the p−n junction geometry of the lateral NWs compared to the NWs in a vertical

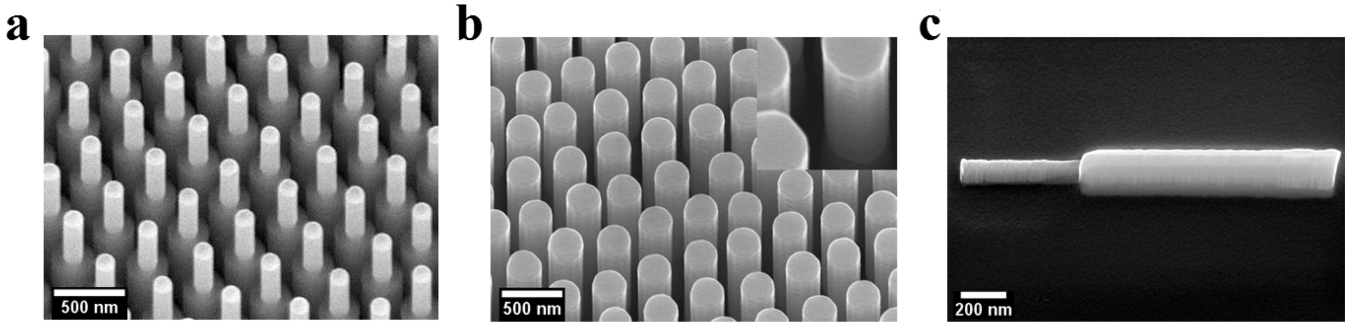

Figure 2. (a) SEM image of InP NW cores with partially etched oxide shell, before InP shell growth. (b) SEM image of p−i−n core−shell NWs with shells grown only at the top part of the core. (c) SEM image of a mechanically transferred lateral NW after etching of the oxide shell, semiburied in a transparent resist, ready for the deposition of the contacts.

DOI: 10.1021/nl504559g
Nano Lett. 2015, 15, 1809−1814

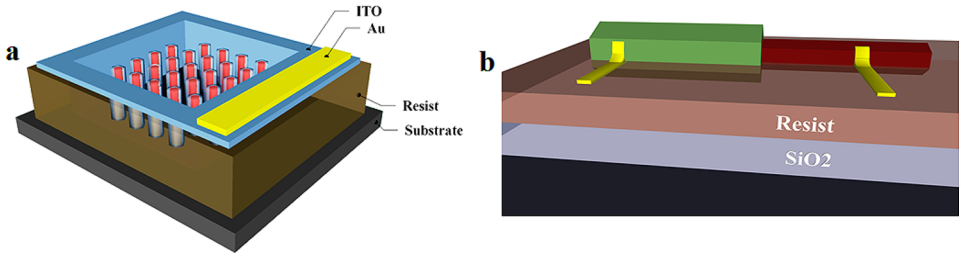

Figure 3. (a) Schematic of an array of vertical InP core−shell NWs, contacted with ITO and configured as a 100 × 100 μm^2 PV device. (b) Schematic of a contacted lateral single NW PV device on a SiO_2-coated substrate, semiburied in a transparent resist.

array. An SEM image of a lateral NW after etching of the bottom oxide shell is shown in Figure 2c. Spectrally resolved room-temperature photocurrent measurements, done on the grown NWs, closely mimicked the photocurrent associated with a reference planar InP p−i−n sample (see Supporting Information Figure S1). This resemblance indicates that the crystal structure of the grown NWs is predominantly zincblende.[21]

In order to fabricate PV devices from the vertical NW arrays, a resist lifting layer was first patterned on the samples by UV lithography to define a 100 × 100 μm^2 device area and to form a flat surface for probing (see Figure 3a for the device schematic). NWs were then contacted by 150 nm of sputtered indium tin oxide (ITO) as a transparent top contact, whereas the p-type substrate was used as the back contact. A 300 nm thick gold pad was evaporated on top of the ITO on the lifting layer to enable low resistance electrical probing. For contacting single NWs as lateral PV devices, the grown NWs were etched in a buffered HF solution to remove the oxide at the bottom segment of the cores and then mechanically transferred to a Si substrate, which was coated with a layer of SiO_2. Etching the oxide, surrounding the bottom segment of the cores, enabled access to the cores for electrical contacting. Next the transferred NWs were buried in a transparent resist, which was subsequently thinned down with RIE to enable a continuous contact deposition on the NWs.[22] Using electron beam lithography (EBL) and metal evaporation, Pd(2 nm)/Zn(20 nm)/Pd(10 nm)/Au(100 nm) contacts were defined on the lateral NWs for electrical probing. Figure 3b depicts a schematic of a contacted lateral single NW PV device.

It can be shown that for our NW geometry with a 1.1 μm long, top radial junction segment in an array with 400 nm pitch almost all the absorption takes place at the top 1.1 μm part (see Supporting Information Figure S2). If we had chosen to have a radial junction much longer than 1.1 μm, we would have had virtually unilluminated segments at the bottom of vertical NWs that would have made the comparison with a totally illuminated lateral NW unreasonable. On the other hand, reducing the junction length below the effective absorption depth reduces the short-circuit current associated with a vertical NW by decreasing the illuminated junction volume. Tailoring the junction length to the effective absorption depth has a benefit of reducing reverse saturation current as well, which subsequently increases the open-circuit voltage.[23]

Vertical NW array samples as well as lateral single NW devices were characterized under 1 sun, AM1.5G, 100 mW/cm^2 solar spectrum illumination at room temperature. Figure 4 shows the dark and illuminated $I-V$ characteristics of the vertically and laterally oriented devices with the highest measured short-circuit current (I_{sc}). The $I-V$ characteristics of the vertical array device shown in the figure are normalized

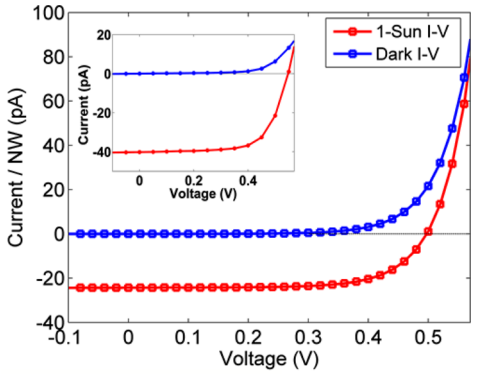

Figure 4. Normalized $I-V$ characteristics of the vertical array PV device with the highest short-circuit current (I_{sc}) in dark and under 1 sun illumination. Inset shows the corresponding $I-V$ characteristics associated with the lateral single PV device having the highest measured I_{sc}.

to the number of NWs in contact in a 100 × 100 μm^2 device area. As it can be seen in Figure 4, the I_{sc} of the lateral device is almost 1.7 times larger than that of the average I_{sc} of individual NWs in the vertical array device. The I_{sc} per NW measured on 22 vertical array devices was found to have an average of 22.5 pA with a standard deviation of 1.9 pA, while the I_{sc} measured on 5 lateral single devices was found to fall between 37.2 and 43.8 pA with an average value of 40.4 pA. The ratio of the I_{sc} of lateral devices to the normalized I_{sc} of vertical devices determined to be in the range between 1.46 and 2.07. The efficiency measured on the vertical array device with the highest I_{sc} was 5.3% with J_{sc} = 15.7 mA/cm^2, V_{oc} = 0.50 V and FF = 67.7%. For calculating the efficiency of the lateral NW PV device with the best performance, we used the geometrical cross section of the p−i−n junction to approximate the amount of light incident on the NW. The such-calculated efficiency of the lateral NW PV device with the highest I_{sc} was 5.6% with J_{sc} = 13.9 mA/cm^2, V_{oc} = 0.58 and FF = 69.7%. We above chose to compare the I_{sc} of vertically and laterally oriented devices in a direct manner, because I_{sc} is a well-defined quantity. However, it is not as straightforward to compare the efficiencies in laterally and vertically oriented NW PV devices due to the fact that the effective absorption cross section of a lateral NW can differ significantly from its geometrical cross section, considering optical resonance effects.[24]

To better understand our experimental finding that the lateral NWs absorb up to two times more light compared to each vertical NWs in the arrays with 400 nm pitch, we performed electromagnetic modeling of the absorption of light in vertically and laterally oriented NW. The framework for modeling of a lateral single NW was based on the Lorenz-Mie scattering theory of a dielectric cylinder where we thus

DOI: 10.1021/nl504559g
Nano Lett. 2015, 15, 1809−1814

approximated the NW as being infinitely long and surrounded completely by air.[25] The absorption properties of a lateral NW on SiO_2 is expected to differ negligibly from that of a lateral isolated NW completely enclosed by air, considered in the modeling.[26] The contribution of the bottom, core-only, segment of the NWs to I_{sc} was not considered in the simulations due to the short diffusion length of the minority carriers in the highly doped NW cores.[27] The light was considered to be incident at normal angle, that is, perpendicular to the axis of the lateral NWs. To calculate the I_{sc} in the lateral NWs, I_{lat}, we calculated the absorption cross-section $C_{abs}(\lambda)$, which corresponds to the equivalent planar surface area from which a NW can absorb all the incident light at wavelength λ, to yield the modeled absorption (see Supporting Information Figure S3 for the calculated C_{abs}). Next, we assumed that each absorbed photon of the AM1.5G solar spectrum contributes one electron−hole pair to the current. This gives rise to the equation

$$I_{lat} = eL \int_{280nm}^{925nm} \frac{I_{AM1.5}(\lambda)C(\lambda)}{\frac{hc}{\lambda}} d\lambda \quad (1)$$

where e is the elementary charge, h is Planck's constant, c is the speed of light in vacuum, L = 1.1 μm is the length of the radial p−i−n section, and $I_{AM1.5}$ is the AM1.5G intensity spectrum. Here, 925 nm corresponds to the bandgap wavelength of InP and 280 nm corresponds to the low-wavelength limit, below which the AM1.5G spectrum exhibits negligible intensity. For optical modeling of the vertical NW arrays, a scattering matrix method was applied.[28] We considered each NW to have a 0.9 μm long bottom core segment of 130 nm in diameter, and a 1.1 μm long thicker top core−shell segment with 280 nm diameter, as illustrated in Figure 1. A 75 nm thick SiO_2 layer was considered to cover the bottom segments of each NW and the substrate. On top of the SiO_2 layer, a 40 nm thick ITO top layer was considered to cover the substrate as well as the lateral surfaces of the NWs. The ITO thickness was considered to be 150 nm at the top of each NW to account for the higher deposition rate at the top of NWs in the actual ITO sputtering process. Experimentally determined values for refractive indices of InP,[29] ITO,[1] and SiO_2[30] were used in the simulations. In order to calculate the I_{sc} generated in the vertical NWs, I_{ver}, we spatially resolved the absorption occurring in the 1.1 μm long, top radial p−i−n segments with 280 nm diameter.

Our modeling showed that I_{lat} = 82.4 pA whereas I_{ver} = 44.4 pA for a pitch of p = 400 nm corresponding to the fabricated vertical NW PV devices. Thus, in agreement with the experimental observations the modeling showed that the lateral NWs absorb stronger than the corresponding vertical NWs by a factor of I_{lat}/I_{ver} = 1.85, which falls in the range between 1.46 and 2.07, obtained from the experiments. It should be noticed, however, that the experimentally determined mean values of I_{sc} for laterally and vertically oriented NWs were both almost a factor of 2 lower than the values deduced from the modeling. We assign these, experimentally obtained, lower than theoretically expected values to a less than 100% extraction of photogenerated charges, which we attribute to different recombination mechanisms, in particular surface recombination, preventing separation of photogenerated electrons and holes.[3] Quantum efficiencies in the order of 50% have been experimentally observed in other studies as well.[3]

Upon increasing the pitch of the vertical array in our model from p = 400 nm up to p = 2000 nm, we find that the I_{sc} per NW increases initially and then flattens out at large pitches (see Figure 5). The increase in absorption indicates that the NWs,

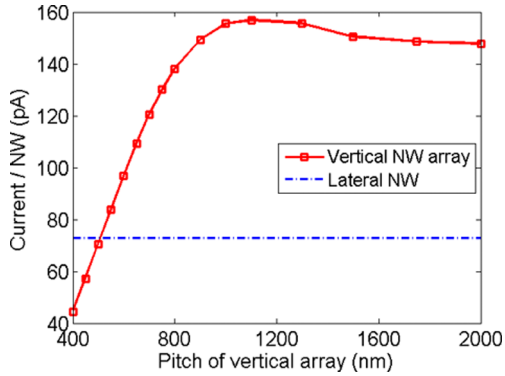

Figure 5. Simulated short-circuit current (I_{sc}) per NW versus pitch (solid red line) of a p−i−n core−shell NW PV device in a vertical array under 1 sun illumination together with the corresponding simulated I_{sc} of a lateral single NW PV device under the same illumination conditions (dashed blue line).

competing with their neighbors to absorb incident photons, get access to a larger number of photons as the pitch increases. As it can be seen in Figure 5, the absorption of the NWs in an array becomes equal to that in the lateral NWs at $p \approx 510$ nm ($I_{lat} = I_{ver}$), and it exceeds this amount as the pitch continues to increase. In other words, depending on the pitch of the array, absorption in the vertical NWs can be lower than, equal to, or higher than that in the lateral NWs. For the largest value of p considered in the simulations (p = 2000 nm), we find that $I_{ver} > 2I_{lat}$, and the I_{sc} per NW settles to a value of $I_{ver} \approx 150$ pA. This independence of I_{ver} from the pitch for large values of p is expected considering that internanowire coupling diminishes as the separation between the NWs increases. At large separation distances, neighboring NWs no longer compete to absorb incident photons. Figure 5 also indicates that the absorption per NW in the vertical array is slightly higher at p = 1000 nm compared to the absorption at p = 2000 nm. If we consider that the absorption at p = 2000 nm separation corresponds closely to the case of a single isolated vertical NW, we can conclude that at p = 1000 nm, the NWs scatter light into each other in such a manner that the absorption is enhanced compared to a single isolated vertical NW.

As shown above, a NW in a vertical array with p = 2000 nm generates a much larger photocurrent compared to a NW in a vertical array with p = 400 nm. However, we should consider that increasing the NW separation decreases the number of NWs per unit area, and this can subsequently reduce the overall device short-circuit current density, J_{sc}, which is an important figure of merit for the performance of a solar cell. In order to find the optimum pitch, which yields the maximum J_{sc}, we calculated the current density versus array pitch for our NW structure, as depicted in Figure 6. As it can be seen in the figure, there is a maximum with J_{sc} = 28.2 mA/cm^2 at $p \approx 500$ nm. Considering that the maximum possible value of J_{sc} is 34.5 mA/cm^2 for an InP single-junction PV device,[1] the radial p−i−n junctions of the vertical NWs with p = 500 nm can absorb more than 80% of the available photons (see Supporting Information Figure S4a for spectrally resolved absorption spectra where values in excess of 80% are obtained for a large part of the

DOI: 10.1021/nl504559g
Nano Lett. 2015, 15, 1809−1814

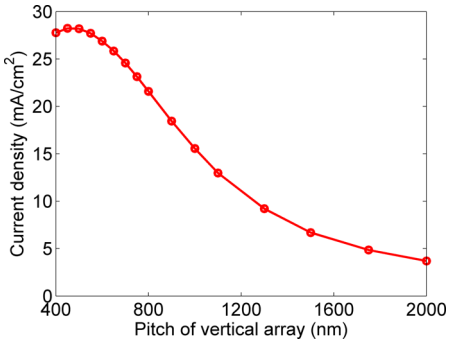

Figure 6. Simulated short-circuit current density of a vertical InP core−shell NW array versus array pitch calculated under 1 sun illumination.

visible spectrum). It should be noticed that in the present geometry, we employ the HE_{12} and HE_{13} waveguide resonances in the individual NWs to enhance the absorption[11] (see Supporting Information Figure S4b). The absorption could possibly be further increased if the NW diameter is tuned for an even more optimized use of these absorption resonaces.[11,31,32]

In summary, a joint experimental−theoretical approach was applied to quantitatively compare the absorption in InP core−shell NW PV devices in lateral and vertical orientation. The presented method could primarily be used to evaluate how accurately a laterally oriented single NW PV device can represent a NW in a vertical array device. The optical modeling revealed that the array pitch plays a determining role in a comparative study of absorption in that depending on the pitch, absorption in a vertical NW in an array could be lower than, equal to, or higher than that in a lateral single NW with the same dimensions. Increasing the pitch results in increased absorption per NW, but on the other hand it reduces the number of NWs per unit area, which can subsequently reduce the overall short-circuit current density of a vertical array device. These two conflicting requirements should be considered in the design of the pitch in vertical array PV devices to obtain an optimum performance in a certain NW geometry.

■ ASSOCIATED CONTENT

Supporting Information

Spectrally resolved photocurrent measurements on the grown NWs together with the photocurrent from a reference zincblende sample, simulated short-circuit current per NW associated with the top radial junction and the bottom core-only segments, and modeled absorption cross sections in vertical and lateral NWs. This material is available free of charge via the Internet at http://pubs.acs.org.

■ AUTHOR INFORMATION

Corresponding Author

*E-mail: lars.samuelson@ftf.lth.se.

Notes

The authors declare no competing financial interest.

■ ACKNOWLEDGMENTS

The authors gratefully acknowledge Dr. Ingvar Åberg from Sol Voltaics AB, Sweden, for fruitful discussions and for assistance with the electro-optical measurements. This work was supported by the Nordic innovation program NANORDSUN, Swedish Research Council (VR), the Swedish Foundation for Strategic Research (SSF), the Swedish Energy Agency, the Nanometer Structure Consortium at Lund University (nmC@LU), and the Knut and Alice Wallenberg Foundation.

■ REFERENCES

(1) Wallentin, J.; Anttu, N.; Asoli, D.; Huffman, M.; Åberg, I.; Magnusson, M. H.; Siefer, G.; Fuss-Kailuweit, P.; Dimroth, F.; Witzigmann, B.; Xu, H. Q.; Samuelson, L.; Deppert, K.; Borgström, M. T. *Science* **2013**, *339* (6123), 1057−1060.
(2) Tian, B.; Zheng, X.; Kempa, T. J.; Fang, Y.; Yu, N.; Yu, G.; Huang, J.; Lieber, C. M. *Nature* **2007**, *449* (7164), 885−889.
(3) Yoshimura, M.; Nakai, E.; Tomioka, K.; Fukui, T. *Applied Physics Express* **2013**, *6* (5), 052301.
(4) Mariani, G.; Zhou, Z.; Scofield, A.; Huffaker, D. L. *Nano Lett.* **2013**, *13* (4), 1632−1637.
(5) Nakai, E.; Yoshimura, M.; Tomioka, K.; Fukui, T. *Jpn. J. Appl. Phys.* **2013**, *52* (5R), 055002.
(6) Heurlin, M.; Wickert, P.; Fält, S.; Borgström, M. T.; Deppert, K.; Samuelson, L.; Magnusson, M. H. *Nano Lett.* **2011**, *11* (5), 2028−2031.
(7) Mårtensson, T.; Svensson, C. P. T.; Wacaser, B. A.; Larsson, M. W.; Seifert, W.; Deppert, K.; Gustafsson, A.; Wallenberg, L. R.; Samuelson, L. *Nano Lett.* **2004**, *4* (10), 1987−1990.
(8) Anttu, N. *Opt. Lett.* **2013**, *38* (5), 730−732.
(9) Anttu, N.; Xu, H. *J. Nanosci. Nanotechnol.* **2010**, *10* (11), 7183−7187.
(10) Cao, L.; Fan, P.; Vasudev, A. P.; White, J. S.; Yu, Z.; Cai, W.; Schuller, J. A.; Fan, S.; Brongersma, M. L. *Nano Lett.* **2010**, *10* (2), 439−445.
(11) Anttu, N.; Xu, H. *Opt. Express* **2013**, *21* (103), A558−A575.
(12) Hu, L.; Chen, G. *Nano Lett.* **2007**, *7* (11), 3249−3252.
(13) Kim, S.-K.; Day, R. W.; Cahoon, J. F.; Kempa, T. J.; Song, K.-D.; Park, H.-G.; Lieber, C. M. *Nano Lett.* **2012**, *12* (9), 4971−4976.
(14) Kempa, T. J.; Cahoon, J. F.; Kim, S.-K.; Day, R. W.; Bell, D. C.; Park, H.-G.; Lieber, C. M. *Proc. Natl. Acad. Sci. U.S.A.* **2012**, *109* (5), 1407−1412.
(15) Christesen, J. D.; Zhang, X.; Pinion, C. W.; Celano, T. A.; Flynn, C. J.; Cahoon, J. F. *Nano Lett.* **2012**, *12* (11), 6024−6029.
(16) Kayes, B. M.; Atwater, H. A.; Lewis, N. S. *J. Appl. Phys.* **2005**, *97* (11), 114302.
(17) Colombo, C.; Heiβ, M.; Grätzel, M.; Morral, A. F. *Appl. Phys. Lett.* **2009**, *94* (17), 173108−173108−3.
(18) Heurlin, M.; Hultin, O.; Storm, K.; Lindgren, D.; Borgström, M. T.; Samuelson, L. *Nano Lett.* **2014**, *14* (2), 749−753.
(19) Wagner, R.; Ellis, W. *Appl. Phys. Lett.* **1964**, *4* (5), 89−90.
(20) Kawaguchi, K.; Heurlin, M.; Lindgren, D.; Borgström, M. T.; Ek, M.; Samuelson, L. *Appl. Phys. Lett.* **2011**, *99* (13), 131915.
(21) Jain, V.; Nowzari, A.; Wallentin, J.; Borgström, M. T.; Messing, M. E.; Asoli, D.; Graczyk, M.; Witzigmann, B.; Capasso, F.; Samuelson, L.; Pettersson, H. *Nano Res.* **2014**, *7* (4), 1−9.
(22) Storm, K.; Halvardsson, F.; Heurlin, M.; Lindgren, D.; Gustafsson, A.; Wu, P. M.; Monemar, B.; Samuelson, L. *Nat. Nanotechnol.* **2012**, *7* (11), 718−722.
(23) Yu, S.; Kupec, J.; Witzigmann, B. *J. Comput. Theor. Nanosci.* **2012**, *9* (5), 688−695.
(24) Cao, L.; White, J. S.; Park, J.-S.; Schuller, J. A.; Clemens, B. M.; Brongersma, M. L. *Nat. Mater.* **2009**, *8* (8), 643−647.
(25) Bohren, C. F.; Huffman, D. R. *Absorption and Scattering of Light by Small Particles*; John Wiley & Sons: New York, 2008.
(26) Heiss, M.; i Morral, A. F. *Appl. Phys. Lett.* **2011**, *99* (26), 263102.
(27) Wallentin, J.; Wickert, P.; Ek, M.; Gustafsson, A.; Wallenberg, L. R.; Magnusson, M. H.; Samuelson, L.; Deppert, K.; Borgström, M. T. *Appl. Phys. Lett.* **2011**, *99* (25), 253105.
(28) Anttu, N.; Xu, H. *Phys. Rev. B* **2011**, *83* (16), 165431.
(29) Edwards, F. *Handbook of Optical Constants of Solids*, Palik, E. D., Ed.; Academic Press: New York, 1985; Vol. *1*, pp 547−569.

DOI: 10.1021/nl504559g
Nano Lett. 2015, 15, 1809−1814

(30) Philipp, H. *Handbook of Optical Constants of Solids*, Palik, E. D., Ed.; Academic Press: New York, 1985; Vol. *1*, pp 749−763.
(31) Kupec, J.; Stoop, R. L.; Witzigmann, B. *Opt. Express* **2010**, *18* (26), 27589−27605.
(32) Huang, N.; Lin, C.; Povinelli, M. L. *J. Opt.* **2012**, *14* (2), 024004.

DOI: 10.1021/nl504559g
Nano Lett. 2015, 15, 1809−1814